BIOLOGY OF REPRODUCTION (2016) **94**(2):41, 1–12
Published online before print 13 January 2016.
DOI 10.1095/biolreprod.115.136358

Ggnbp2 Is Essential for Pregnancy Success via Regulation of Mouse Trophoblast Stem Cell Proliferation and Differentiation[1]

Shengqiang Li,[4] Andrew K. Moore,[4] Jia Zhu,[4] Xian Li,[4] Huaxin Zhou,[5] Jing Lin,[4] Yan He,[4] Fengying Xing,[4] Yangbin Pan,[4] Henry C. Bohler,[4] Jixiang Ding,[5] Austin J. Cooney,[6] Zijian Lan,[3,7] and Zhenmin Lei[2,4]

[4]*Department of OB/GYN & Women's Health, University of Louisville School of Medicine, Louisville, Kentucky*
[5]*Birth Defects Center, Department of Molecular, Cellular and Craniofacial Biology, University of Louisville School of Dentistry, Louisville, Kentucky*
[6]*Department of Molecular and Cellular Biology, Baylor College of Medicine, One Baylor Plaza, Houston, Texas*
[7]*Division of Life Sciences and Center for Nutrigenomics & Applied Animal Nutrition, Alltech Inc., Nicholasville, Kentucky*

ABSTRACT

The *Ggnbp2* null mutant embryos died in utero between Embryonic Days 13.5 to 15.5 with dysmorphic placentae, characterized by excessive nonvascular cell nests consisting of proliferative trophoblastic tissue and abundant trophoblast stem cells (TSCs) in the labyrinth. Lethality of *Ggnbp2* null embryos was caused by insufficient placental perfusion as a result of remarkable decreases in both fetal and maternal blood vessels in the labyrinth. These defects were accompanied by a significant elevation of *c-Met* expression and phosphorylation and its downstream effector Stat3 activation. Knockdown of *Ggnbp2* in wild-type TSCs in vitro provoked the proliferation but delayed the differentiation with an upregulation of *c-Met* expression and an enhanced phosphorylation of c-Met and Stat3. In contrast, overexpression of *Ggnbp2* in wild-type TSCs exhibited completely opposite effects compared to knockdown TSCs. These results suggest that loss of GGNBP2 in the placenta aberrantly overactivates c-Met-Stat3 signaling, alters TSC proliferation and differentiation, and ultimately compromises the structure of placental vascular labyrinth. Our studies for the first time demonstrate that GGNBP2 is an essential factor for pregnancy success acting through the maintenance of a balance of TSC proliferation and differentiation during placental development.

c-Met, Ggnbp2*, knockout, labyrinth, placenta, Stat3, trophoblast stem cells*

INTRODUCTION

The placenta is an indispensable chimeric organ that supports mammalian embryonic development [1]. The organization of the murine placenta is morphologically and functionally divided into two major components, namely the junctional and labyrinth zones. The junctional zone is composed of the outermost primary trophoblast giant cells (TGCs) and glycogen trophoblasts that directly interact with maternal decidual and spongiotrophoblast (SpT) cells, forming a distinct cellular layer overlaying the labyrinth zone. The junctional zone is known to be involved in implantation, structural support, and secretion of peptide hormones. The labyrinth zone is the inner compartment proximal to the fetus. It consists of maternal blood spaces and fetal capillaries separated by a trilaminar layer of trophoblast, including two layers of multiple nuclear syncytiotrophoblasts (SynTs) surrounding the fetal blood vessel endothelial cells and a layer of sinusoidal TGCs lining the maternal blood sinus. The most important function of the labyrinth is for the transport of nutrients, gasses, ions, hormones, as well as waste between the mother and fetus [1–3]. The flexuous network of maternal and fetal vessels in the labyrinth is established at Embryonic Day 10.5 (E10.5) [4, 5]. With advanced gestation, it undergoes extensive modifications so that the exchange surfaces of the maternal-fetal interface are greatly expanded to meet the demands of the growing fetus. Impairment of labyrinth transport function in the majority of gene mutations results from a small labyrinth [2].

The placenta is derived from the outer single layer of cells of the blastocyst called the trophectoderm. The mural trophectoderm that is away from the inner cell mass (ICM) undergoes differentiation and DNA endoreduplication to form primary TGCs, while the polar trophectoderm that is close to the ICM gives rise to trophoblast stem cells (TSCs) that subsequently forms the extraembryonic ectoderm and ultimately develops into the SpT layer and all types of trophoblasts in the labyrinth [1, 6]. The fetal vascular endothelial cells in the labyrinth evolve from the ICM-originated extraembryonic mesoderm [3, 4]. Accumulated data from the last decade indicate that the morphogenesis and functional capacity of the placenta are highly dependent on the precise regulation of TSC decisions to expand or to differentiate. TSC decisions are known to be influenced by a number of molecules, including transcription factors, epigenetic modifiers, and metabolic regulators [1, 7–9]. For example, Eomes, Esrrb, Cdx2, and Stat3 (signal transducers and activators of transcription 3) are essential for sustenance of TSC renewal and stemness, whereas

[1]This work was supported in part by Grants R01-HD057501 (Z.M.L.), 5P20RR017702-10, and 8P20 GM103453-10, and project I (Z.J.L.) from the National Institutes of Health. Presented in part at the Society for Gynecologic Investigation 60th Annual Meeting, 23 March 2013, Orlando, Florida.
[2]Correspondence: Zhenmin Lei, Department of OB/GYN, 412 A Building, 500 S Preston St., University of Louisville HSC, Louisville, KY 40202. E-mail: zhenmin.lei@louisville.edu
[3]Correspondence: Zi-Jian Lan, Division of Life Sciences, Center for Nutrigenomics & Applied Animal Nutrition, Alltech Inc., 3031 Catnip Hill Road, Lexington, KY 40356. E-mail: zlan@alltech.com

Received: 16 October 2015.
First decision: 16 November 2015.
Accepted: 7 January 2016.

eISSN: 1529-7268 http://www.biolreprod.org
ISSN: 0006-3363

Mash2, Tpbpa, Hand1, and Gcm1 are necessary for TSC differentiation toward specific lineages of trophoblasts [10–13]. It is also clear now that the cell fate decisions of TSCs are influenced by numerous extracellular signals that affect the activities of the family of receptor tyrosine kinases (RTK), Jak kinase, Smad, Notch, and Wnt pathways [6, 8, 14, 15]. Emerging evidence suggests that extensive interactions of these extracellular signals and intracellular factors are critical to balance TSC renewal and differentiation during normal placental development.

The RTK family includes c-Met, which dimerizes and induces autophosphorylation of tyrosine residues Y1234 and Y1235 after binding to hepatocyte growth factor (HGF) or as a result of cross talk with other signaling molecules [16, 17]. Subsequently, c-Met undergoes additional tyrosine phosphorylation and activates diverse downstream signaling pathways, including Src-Stat3, PI3K-PDK1, and Raf-MAPK cascades, to exert multiple biological activities such as sustaining cell proliferation, survival, invasion, and stemness in a context-dependent and tissue-specific manner [18, 19]. Signaling by c-Met is crucial for sustaining proliferation of multipotent labyrinth trophoblast progenitors during midgestation and is essential for establishing the functional placental exchange interface [15].

Gametogenetin-binding protein 2 (GGNBP2, also known as ZFP403, ZNF403, DIF3, LCRG1, and LZK1) is encoded by a gene consisting of 15 exons in human chromosome 17. The murine ortholog is in chromosome 11. It is evolutionarily conserved across humans, mice, and rats, sharing 87% homology in nucleotide sequence and 96% homology in amino acid sequence between humans and mice. The full length murine GGNBP2 protein is composed of 740 amino acids. It contains a Cys2His2 (C2H2) zinc finger motif at the N-terminus and a Leu-X-X-Leu-Leu (LxxLL) nuclear receptor-binding domain at the C-terminus [20–24]. It was originally identified as dioxin-induced factor 3 (DIF3) in mouse embryonic stem cells (ESCs) in 2001 [20]. *Ggnbp2* mRNA transcripts have been detected in a number of tissues, such as testis, heart, brain, lung, liver, kidney, pancreas, placenta, and skeletal muscle [20–23, 25]. The protein was reported to localize in the nucleus as well as the cytoplasm [20, 22]. GGNBP2 has been shown to interact with a testicular protein gametogenetin and is hence known as gametogenetin-binding protein 2 (GGNBP2) [22]. In humans, a shorter form of GGNBP2 containing 288 amino acids at the N-terminal has been reported and named laryngeal carcinoma-related protein 1 (LCRG1) by virtue of it being remarkably down-regulated in primary laryngeal carcinomas and several other human cancer cell lines [21, 22, 24]. It has been speculated that *Ggnbp2* may play a role in spermatogenesis and tumorigenesis. However, the function of *Ggnbp2* in vivo is virtually unknown.

In this study, we generated a *Ggnbp2* knockout mouse line, designated as *Ggnbp2KO,* and demonstrated that GGNBP2 is a novel regulator in mouse TSCs for normal placental labyrinth development and that loss of *Ggnbp2* in TSCs causes aberrant overactivation of c-Met-Stat3 signaling, resulting in a dysregulation of trophoblast proliferation and differentiation. These findings may advance our understanding of normal placental development and pregnancy conditions associated with faulty placental perfusion.

MATERIALS AND METHODS

Animals

A gene-trap ESC clone (clone number IST12476F10 in the C57BL/6 background) with the insertion of a gene-trap vector *LacZ*/*Neo* cassette into the intron between exons 7 and 8 of the *Ggnbp2* allele was used to generate the mutant mice. These correctly targeted ESCs were microinjected into mouse blastocysts by the Texas Institute for Genomic Medicine (College Station, TX) to generate chimeric mice. After the breeding of the chimeric mice with wild-type (Wt) C57BL/6 mice in the Texas Institute for Genomic Medicine, *Ggnbp2* mutant heterozygotes (in the pure C57BL/6 background) were obtained and then transferred to the University of Louisville.

For genotyping the *Ggnbp2* mutant mice, genomic DNA was isolated from the yolk sac, ear notches of embryos, or tail clips of 21-day-old mice using ZR Genomic DNA-Tissue Mini Prep kits according to the procedure recommended by the manufacture (Zymo Research Corp., Irvine, CA). PCR analysis of the genomic DNA was performed to determine the genotype of this mutant mouse line. The Wt *Ggnbp2* allele was determined using PCR primers P1 (5′-AGTGCCATTTACCCACCAAG-3′) and P3 (5′-GAAAGGAGGAGG GAAAGGAA-3′), while the *Ggnbp2* null allele were determined using PCR primers P1 and P2 (5′-GACAGTATCGGCCTCAGGAAGATCG-3′) (Supplemental Fig. S1; Supplemental Data are available online at www.biolreprod.org). To determine how effective the gene trap was in terminating transcription, we used RT-PCR with the primer pair P4 and P5 (Supplemental Fig. S1 and Table S1).

For timed matings, adult *Ggnbp2* mutant heterozygous females and males were paired. The day on which a copulation plug was evident was designated as E0.5 of pregnancy. Pregnant females were sacrificed, and blastocysts (E3.5), fetuses, and placentae at different gestation stages (E10.5–E18) were collected. Viable fetuses (determined by positive heartbeat) were counted and placental weights were recorded. The gross appearance of fetuses and placentae were carefully examined under a dissecting microscope.

The animals were housed under 12L:12D cycles with food and water provided ad libitum. The studies have been approved by the Animal Care and Use Committee of the University of Louisville. All the mice were euthanized under ketamine anesthesia, and all efforts were made to minimize their discomfort.

Transplacental Passage of Rhodamine 123

The procedure was performed as described by Dupressoir et al. [26]. Briefly, timed pregnant mice at E15.5 received a single intraperitoneal injection of rhodamine 123 (1 mg/kg body weight; Sigma, St Louis, MO). The mice were killed 2 h after the injection, and living embryos were analyzed with an Olympus fluorescence stereomicroscope. Each embryo tail was clipped for determination of the genotype by PCR.

Histology and Morphometric Analysis of Labyrinth Vessels

Placentae were fixed in 4% paraformaldehyde in phosphate-buffered saline (PBS) overnight and embedded in paraffin. Serial 5 μm thick cross-sections were cut and used for hematoxylin and eosin, histochemistry, and immunochemistry staining.

To define maternal and fetal vessels in the labyrinth, a double staining of maternal vessels by alkaline phosphatase histochemistry and fetal vessels by laminin immunohistochemistry were performed. Briefly, deparaffinized placental slides were treated with 0.1 M Tris-HCl buffer (pH 9.5) containing 1% Tween 20, 0.05 M $MgCl_2$, and 0.15 M NaCl and then incubated with 5-bromo, 4-chloro, 3-indolylphosphate /nitro-blue tetrazolium substrate solution to detect the alkaline phosphatase-positive cell lining of maternal vessels. The slides were subsequently incubated with laminin antibody to detect the laminin-positive cell lining of fetal vessels by immunohistochemistry as described below. Morphometric analysis of labyrinth vascular areas was performed on digital images on a computer screen captured by an Olympus microscope equipped with a digital camera. The areas (μm^2) of labyrinth, maternal vessel (blue color outlined), and fetal vessel (brown color outlined) were quantitatively measured using imaging application software, MicroSuite version 5 (Olympus Soft Imaging Solution Corp., Lakewood, CO). In all cases, the central region of the placenta was examined because this is where the morphology is well defined and most consistent [27]. An average of five nonconsecutive sagittal sections at an interval of at least 40 μm for each placenta was used for the measurement. The results were expressed as a percentage of the labyrinth area.

Cell Proliferation Assays

In vivo bromodeoxyuridine (BrdU) incorporation was used for in situ detection of cell proliferation in the placentae. Briefly, timed pregnant mice at E15.5 received a single intraperitoneal injection of BrdU (100 mg/kg body weight, Sigma) and were killed 2 h after the injection. The placentae were fixed in 10% buffered formalin and embedded in paraffin. BrdU-labeled cells were

detected by immunohistochemistry. The brown-colored nuclei and the labyrinth areas were measured using imaging application software, MicroSuite version 5 (Olympus Soft Imaging Solution Corp.) under a bright field microscope. An average of five nonconsecutive sagittal sections at an interval of at least 40 μm for each placenta was counted. The results were expressed as a percentage of the labyrinth area.

The cell proliferation of TSCs in vitro was measured using CellTiter 96 Aqueous One Solution MTS Cell Proliferation Colorimetric Assay kits following the protocol recommended by the manufacturer (Promega Corp., Madison, WI). TSCs were seeded in 96-well plates at an initial density of 5×10^3 cells/well suspended in TSC growth medium (see below). These cells were cultured for 1, 2, 3, 4, 6, 8, and 10 days for the measurement of the absorbance at 490 nm using a microplate reader.

TdT-Mediated dUTP Nick-End Label Assays

TdT-mediated dUTP nick-end label (TUNEL) staining was performed on formalin-fixed and paraffin-embedded placental sections using an in situ cell death detection Kit (Roche Applied Science, Indianapolis, IN) according to the procedure suggested by the manufacturer. The blue-colored nuclei of apoptotic cells in all the placental sections were visualized and photographed under a bright-field microscope.

Tube Formation Assay

Ggnbp2KO and Wt E15.5 placentae were trimmed free of attached fetal membranes and washed extensively in PBS to remove blood contamination. Each placenta was cut into 15–20 pieces and cultured in 1 ml/well of phenol red-free Dulbecco-modified Eagle medium (DMEM) (Invitrogen, Grand Island, NY) without serum in a 12-well plate for 24 h. The conditioned medium was collected and centrifuged to remove cellular debris.

The effect of placenta conditioned medium on tube formation of human umbilical vein endothelial cells (HUVECs) (ATCC, Manassas, VA) in vitro was carried out by using an endothelial tube formation assay kit (Cell Biosciences Inc., San Diego, CA) according to the procedure recommended by the manufacturer. Briefly, HUVECs suspended in the conditioned medium and 0.5% of fetal bovine serum (FBS) or the conditioned medium diluted with fresh DMEM at 1:1 ratio and 0.5% FBS were seeded to a density of 10 000 cells/well on extracellular matrix gel in a 96-well plate. The results were evaluated 8 and 18 h later under a microscope.

Derivation and Culture of Mouse TSCs from Wt Blastocysts

TSCs were derived from Wt E3.5 blastocysts following the procedure described by Chiu et al. [28]. Briefly, one blastocyst per well were placed in a 12-well plate with mitomycin C-treated mouse embryonic fibroblast (MEF) (ATCC) feeder and cultured in TSC medium (RPMI 1640, 100 μM β-mercaptoethanol, 2 mM L-glutamine, and 20% FBS; Sigma) supplemented with 25 ng/ml FGF4 and 1 μg/ml heparin (Sigma) for 5 days. The blastocyst outgrowth was disaggregated and cultured for an additional 5 to 10 days until cell colonies with epithelial sheetlike morphology and a clear colony boundary were observed. The cell colonies at about 50% confluence were dispersed by trypsin and subcultured in TSC growth medium (30% TSC medium, 70% MEF conditioned medium supplemented with 25 ng/ml FGF4, and 1 μg/ml heparin). After two to three passages, the derived TSCs were maintained in TSC growth medium without MEF feeder. The culture medium was replaced every 2 days. The identity of TSCs was verified by determining the expression of TSC markers *Cdx2* and *Esrrb* but lack of TGC markers *Pl-1, Prl2c2,* and *Tpbpa* using RT-PCR. Differentiation of TSCs was induced by plating 1×10^5 TSCs in 60 mm diameter plates and replacing the culture medium 24 h later with 95% RPMI 1640 and 5% FBS.

Generation of TSCs with Stable Overexpression of Exogenous Ggnbp2

The mouse *Ggnbp2* cDNA fragment was obtained by PCR using mouse testicular cDNA as a template and validated by DNA sequencing. The correct full-length *Ggnbp2* cDNA was cloned into *pcDNA 3.1HisC* vector (Invitrogen) to construct the mammalian expression plasmid *pcDNA3-Ggnbp2*. To generate stable *Ggnbp2* overexpression clones, the TSCs were cultured in TSC growth medium to approximately 50% confluence in a 12-well plate and were transfected with 1 μg of either *pcDNA3-Ggnbp2* or *pcDNA3* plasmid (as a control) using Lipofectamine 2000 (Invitrogen). The TSCs were then cultured in TSC growth medium containing 200 μg/ml G418 (Cellgro Molecular Genetics, Manassas, VA) for 14 days. The G418-resistant clones were selected and subcultured for subsequent experiments. The stable transfection and expression of *Ggnbp2* in the TSCs were verified by both RT-PCR and Western-blot analyses.

Generation of Stable Ggnbp2 Knockdown TSCs

To generate stable *Ggnbp2* knockdown clones, the Wt TSCs were cultured in TSC growth medium to approximately 50% confluence in a 12-well plate and were transduced with *Ggnbp2 shRNA* (small hairpin RNA) lentiviruses or scramble *shRNA* lentiviruses (as a control). *Ggnbp2* (sc-145389) and scramble (sc-108080) *shRNA* lentivirus were purchased from Santa Cruz Biotech (Santa Cruz, CA). *Ggnbp2 shRNA* is a pool of three different *shRNA* plasmids. Typically, a mixture of 1×10^5 infectious units of *Ggnbp2 shRNA* or scramble *shRNA* lentiviral particles, 200 μl TSC growth medium, and 5 μg/ml polybrene (Santa Cruz Biotech) was added to the cells in a 12-well plate and incubated overnight. The transduction medium was then cultured in TSC growth medium containing 2 μg/ml puromycin dihydrochloride (Santa Cruz Biotech) for 10 days. The puromycin dihydrochloride-resistant clones were selected and subcultured for subsequent experiments. RT-PCR and Western blot analysis were used to determine the effectiveness of *Ggnbp2 shRNA* in suppressing *Ggnbp2* mRNA and protein levels in TSCs.

RT-PCR

Total RNA was extracted from E10.5 fetal tissues, placentae, and TSCs using Trizol Reagent (Invitrogen) according to manufacturer's instructions. Two microgram total RNA were reverse transcribed into cDNA with random primers (Invitrogen) and avian myeloblastosis virus reverse transcriptase (Promega Corp.). The cDNA was amplified by PCR with the primer sets of the target gene and a housekeeping gene, ribosomal protein large subunit 19 (*Rpl19*). PCR primers, as listed in Supplemental Table S1, were designed according to the sequences obtained from GenBank using the Vector NTI 12.0 program (Invitrogen) and synthesized by Operon Technologies (Alameda, CA). All primers were designed to amplify the products that covered more than one exon. Each PCR-cycle consisted of denaturation for 45 sec at 94°C, annealing for 1 min at 57°C, and extension for 1 min at 72°C. The amplified products were separated by electrophoresis in agarose gels and stained by ethidium bromide. The intensity of specific bands was scanned and semiquantified using the image analysis software TotalLab (Nonlinear USA Inc., Durham, NC). The results were presented as the ratio of target gene over *Rpl19*.

Western Blot Analysis

The placentae were homogenized using a Tissue-Tearor (RPI Corp., Mt. Prospect, IL) in a lysis buffer. Protein aliquots were separated in SDS-PAGE gels, transferred to Immobilon-polyvinylidene fluoride membranes (Millipore, Billerica, MA) and then incubated overnight with antibodies as listed in Supplemental Table S2. Peroxidase-conjugated secondary antibody (1:2000 dilution; Vector Laboratories, Burlingame, CA) was used as the secondary antibody. Immunoblotting signals were detected by the enhanced chemiluminescence (ECL) Western blot detection system (GE healthcare Biosciences, Pittsburgh, PA). All membranes were reblotted with β-actin antibody as the loading control. The intensity of specific bands was scanned using image analysis software TotalLab. The results were presented as the ratio of target protein over β-actin.

Immunohistochemical Staining

The procedure was performed by an avidin-biotin immunoperoxidase method. Briefly, deparaffinized sections were rehydrated and then incubated with H_2O_2. The sections were then incubated with the primary antibodies as listed in Supplemental Table S2 at 4°C overnight and then incubated with biotinylated secondary antibody (1:100 dilution; Vector Laboratories). After rinsing with PBS, sections were incubated with avidin-biotin-horseradish peroxidase complex using a Vectastain ABC kit (Vector Laboratories). Immunostaining was detected by incubation of the sections with the substrate 3′,3-diaminobenzidine. All sections were counterstained with hematoxylin. Replacement of the primary antibody with irrelevant rabbit or mouse immunoglobulin G (IgG) was used as a procedure control. Eomes-positive cells in the Wt and *Ggnbp2* null mutant labyrinths were counted on five nonconsecutive sagittal sections at an interval of at least 40 μm for each placenta. The results were expressed as a percentage of the labyrinth area.

Immunofluorescent Staining

The coverslips of cultured TSCs were fixed in 2% paraformaldehyde. Placentae used for immunofluorescent staining were fixed in 4% paraformalde-

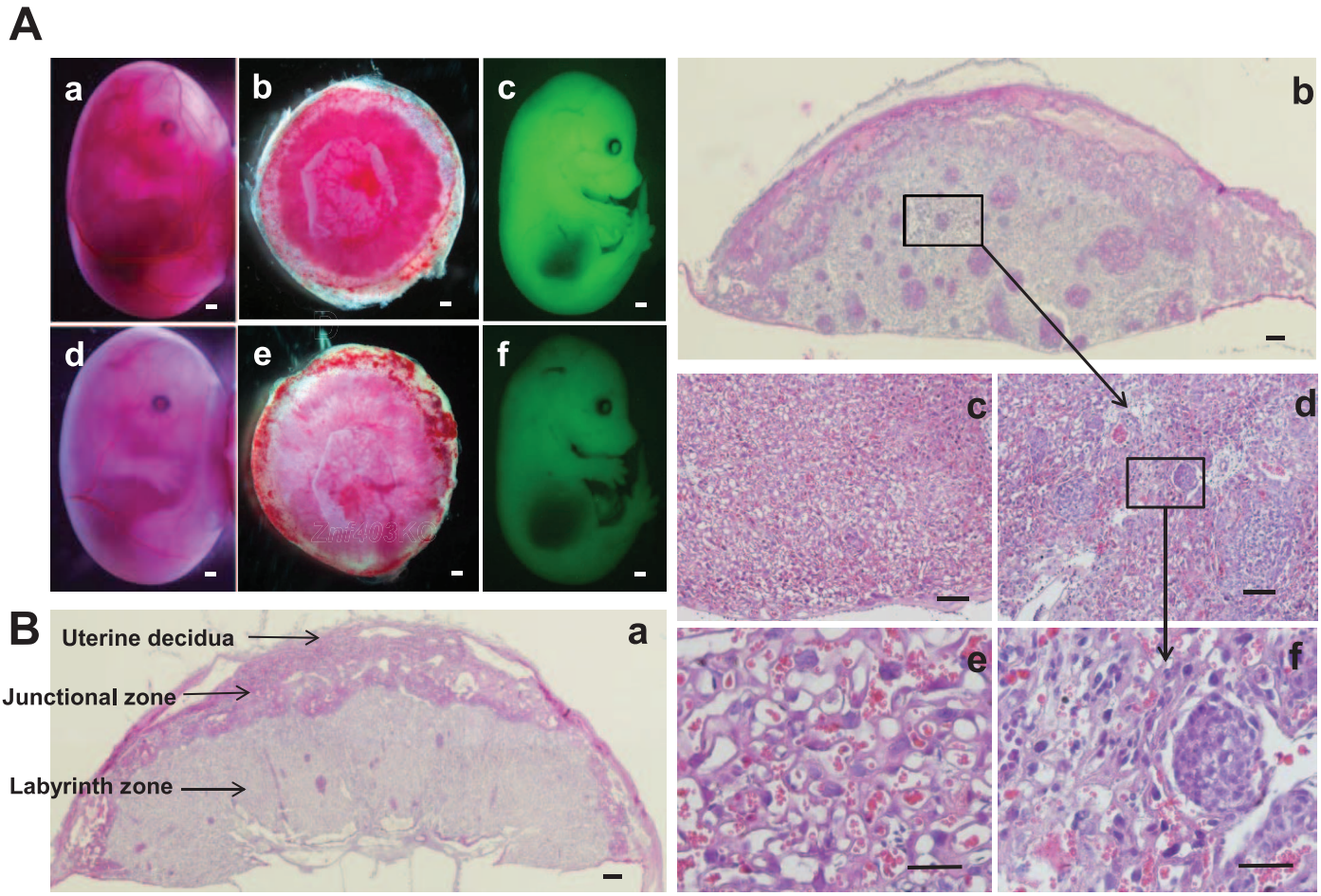

FIG. 1. **A**) Placental abnormalities of *Ggnbp2KO* embryos. Gross appearance of a representative *Ggnbp2KO* E15.5 embryo with yolk sac (**d**) and the placenta (**e**) are slightly paler than their Wt littermate (**a** and **b**). Fluorescent intensity of a representative living *Ggnbp2KO* (**f**) embryo 2 h following an intraperitoneal injection of rhodamine-123 dye into the mother is lower than Wt littermate (**c**). Original magnifications ×5 (**a**–**f**). **B**) Histological appearance of the *Ggnbp2KO* mice show placental defect in the labyrinth layer. Hematoxylin and eosin staining of placental hemisections of E15.5 Wt (**a**, **c**, and **e**) and *Ggnbp2KO* (**b**, **d**, and **f**) embryos reveals that densely packed cell clusters are crowded in the labyrinth layer. The junctional zone, labyrinth zone, and uterine decidua are indicated by arrows in **a**. The labyrinth layer of null mutant placenta (**b**, **d**, and **f**) is more compact and less vascularized areas. Original magnifications ×15 (**a** and **b**), ×40 (**c** and **d**), and ×200 (**e** and **f**). Bar = 10 μm.

hyde, incubated with 30% sucrose in PBS at 4°C, and embedded in optimal-cutting temperature compound. Placental frozen sections and the coverslips of cultured TSCs were permeabilized by 0.01% saponin and then incubated with primary antibodies as listed in Supplemental Table S2 at 4°C overnight. Subsequently, expression of cytokeratin in TSCs and phosphorylated c-Met in the placentae were detected by Texas Red-labeled donkey anti-rabbit IgG (1:100 dilution; Jackson ImmunoResearch, West Grove, PA). The coverslips and frozen placental sections were covered with a 4′,6-diamidino-2-phenylindole-containing mounting medium (Santa Cruz Biotech) to visualize the nuclei. Fluorescent signals on placental section and cultured TSCs were visualized and photographed using an Olympus fluorescence microscope. Replacement of the primary antibody with irrelevant rabbit IgG was used as a procedure control.

Statistical Analysis

The data presented are the means ± SEM. The results were analyzed by one-way analysis of variance and paired Student *t*-test using a version 3.06 Instat program (Graphpad Software, San Diego, CA). $P < 0.05$ was considered statistically significant.

RESULTS

Ggnbp2 *Null Mutant Embryos Are Not Viable*

To investigate the role of GGNBP2 in vivo, we generated a *Ggnbp2* mutant mouse line with targeted disruption of the *Ggnbp2* gene between exons 7 and 8 in the C57BL/6 genetic background using a gene-trap ESC clone (Supplemental Fig. S1). The *LacZ* reporter was not expressed in-frame in this mouse line. Lines with germline transmission were acquired, and subsequent breeding of heterozygous *Ggnbp2* mutant female and male mice resulted in a non-Mendelian ratio at weaning, with no *Ggnbp2* mutant homozygous mice obtained (Supplemental Table S3). Detailed genotyping studies showed that *Ggnbp2* null mutant mice died in utero between E13.5 to E15.5 days (Supplemental Table S3). RT-PCR showed the complete loss of *Ggnbp2* transcripts in null mutant embryos (Supplemental Fig. S1C), indicating that the gene-trap effectively terminated the gene expression. These results suggest that GGNBP2 is essential for normal embryonic development.

Ggnbp2 *Null Mutation Alters the Development of the Placental Labyrinth Zone*

To determine the developmental defects that caused embryo death, we carefully examined the gross anatomy of all the E10.5 to E15.5 embryos from *Ggnbp2* mutant heterozygous male and female matings. Neither deformity of appearance nor malformation of the heart and brain were observed apart from paler embryo and placenta (Fig. 1). The average embryo sizes and placental weights in *Ggnbp2KO* fetuses were comparable

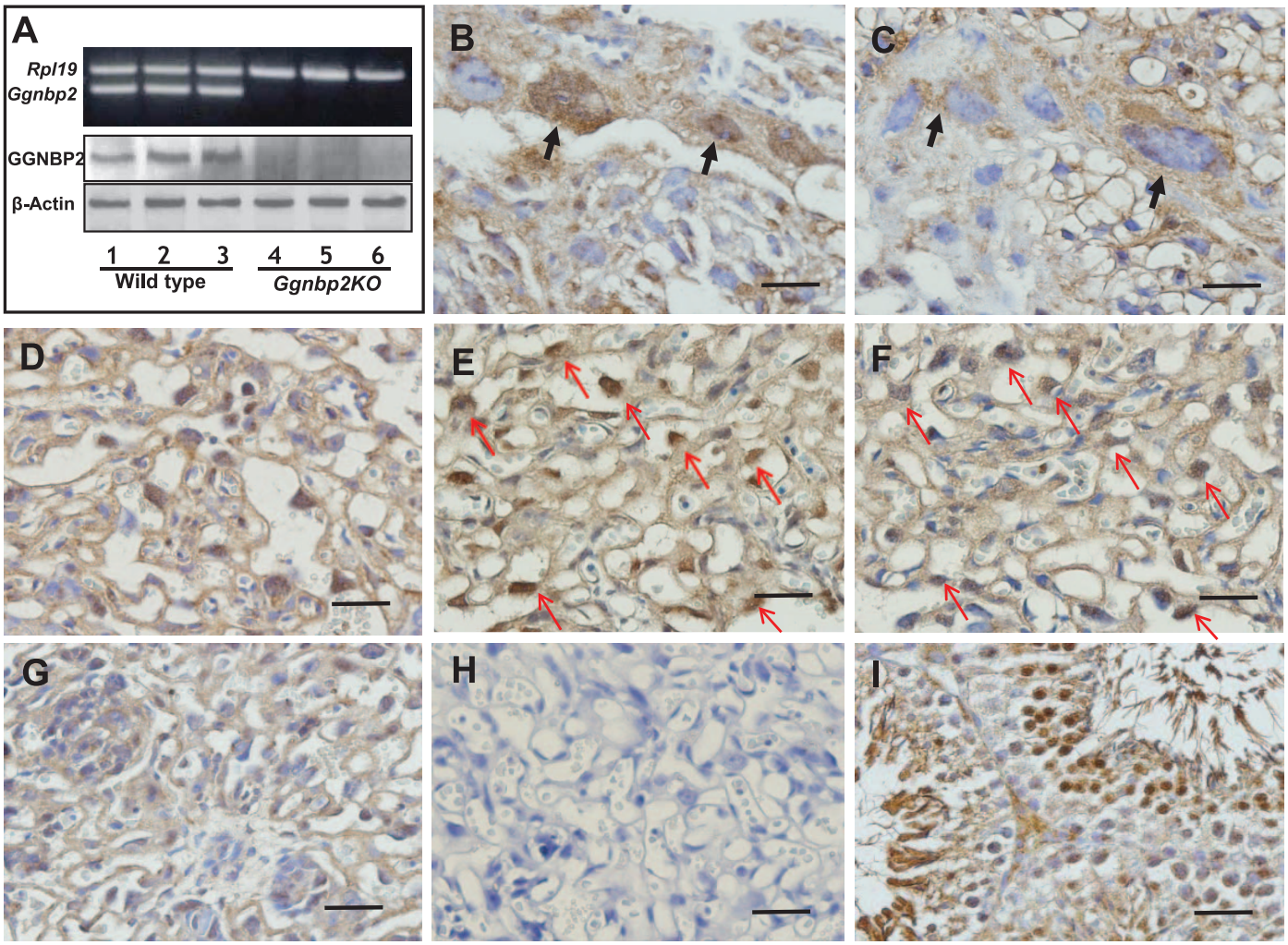

FIG. 2. Expression of *Ggnbp2* in the murine placenta. RT-PCR and Western blot analyses show that both *Ggnbp2* mRNA and protein are readily detectable in E15.5 Wt but are absent in *Ggnbp2KO* placentae (**A**). Immunohistochemical staining with a polyclonal antibody against GGNBP2 in E10.5 (**B** and **D**) and E15.5 (**C** and **E**) Wt placentae show the presence of nuclear staining in primary trophoblast giant cells (TGCs) (black arrows) in E10.5 (**B**) but are absent in the E15.5 (**C**) junctional zone. The immunostaining of GGNBP2 (**D** and **E**) and a labyrinth TGCs marker Hand1 (**F**, red arrows) in adjacent sections shows that GGNBP2 is predominantly localized in labyrinth TGCs (**E**, red arrows). **G**) Representative picture of *Ggnbp2KO* E15.5 placenta showing the lack of GGNBP2 immunostaining in the labyrinth. No GGNBP2 immunostaining in the Wt placenta in which placental sections were incubated with nonrelevant rabbit IgG serves as a procedure control (**H**). Abundant immunostaining of GGNBP2 in the seminiferous tubules of adult mouse testes serves as a positive control (**I**). All sections are counterstained with hematoxylin. Original magnifications ×200 (**B**–**I**). Bar = 10 μm.

to those of Wt siblings. The reason for the relatively normal size and placental weight of *Ggnbp2* null embryos is unknown at the moment.

Histological analyses of midsagittal sections of E10.5, E13.5, and E15.5 placentae showed that the organization of the junctional zone, including primary TGC and SpT layers in *Ggnbp2* null mutant placentae, was similar to the Wt, while an anomalous labyrinth layer was noted in E13.5 and E15.5 placentae. The abnormalities were indistinguishable at E10.5 but very pronounced at E15.5. Therefore, we used living (determined by heart beats) E15.5 placentae for subsequent studies. Unlike Wt embryos, the maternal and fetal vessel spaces in the labyrinth of *Ggnbp2KO* mice were taken up by large densely packed cell aggregates (Fig. 1). However, morphometric analyses using Olympus MicroSuite version 5 software revealed that the areas of the junctional and labyrinth zones were not significantly different between Wt and mutant placentae (data not shown), suggesting that the size of the placenta does not depend on GGNBP2.

Ggnbp2 *Is Expressed in the Placenta*

To gain further clues as to whether the above observed defects of the labyrinth zone of *Ggnbp2KO* placentae is caused by ablation of *Ggnbp2* in the region, we evaluated the expression and the cellular localization of *Ggnbp2* in placenta. First, RT-PCR and Western blots were performed to examine its expression in the whole placenta. As shown in Figure 2, *Ggnbp2* mRNA and its encoded protein were readily detectable in E15.5 Wt but not in *Ggnbp2KO* placentae (Fig. 2A).Then, immunohistochemistry was carried out to determine the cellular localization of GGNBP2 protein in E15.5 placentae. The results revealed that GGNBP2 protein was predominantly localized in primary and labyrinth TGCs. To confirm the identification of the labyrinth TGCs, immunostaining of both GGNBP2 and a labyrinth TGC marker Hand 1 was performed on adjacent placental sections (Fig. 2, E and F). In addition, we also examined the GGNBP2 expression in E10.5 placentae. GGNBP2 appeared to be mainly localized in the nuclei of primary TGCs and disappeared in E15.5 placentae (Fig. 2, B

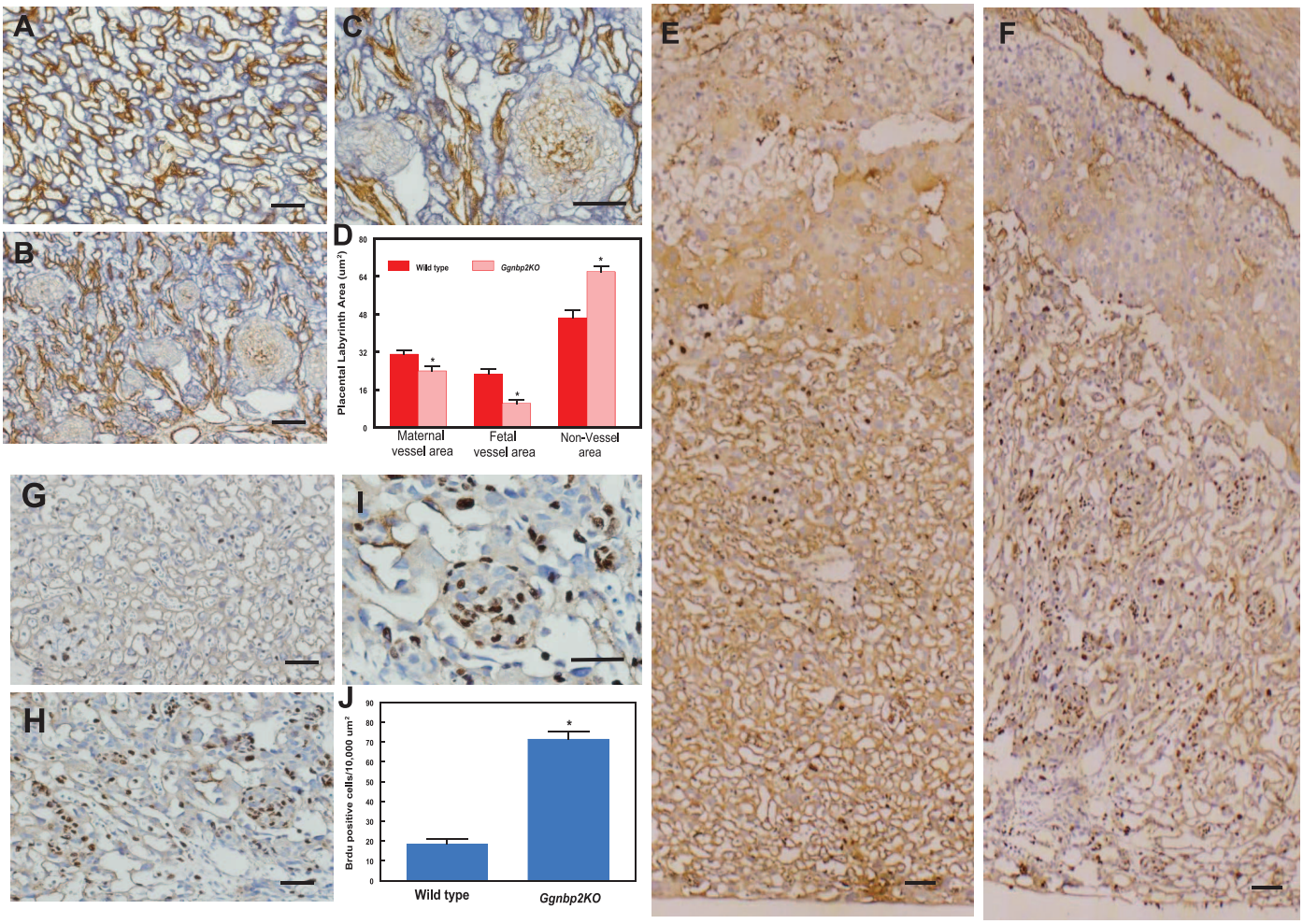

FIG. 3. Effect of *Ggnbp2KO* on vascular spaces in the E15.5 labyrinth (**A**–**D**). Maternal vessels are labeled by alkaline phosphatase histochemistry (blue color), and fetal vessels are labeled by laminin immunohistochemistry (brown color). Maternal and fetal vascular spaces in the null mutant labyrinth are encroached by accumulated cell clusters that are densely packed and alkaline phosphatase negative (**C** and **B**). **D**) The results of quantitative morphometric analyses of maternal and fetal vessel spaces in the labyrinth of Wt and *Ggnbp2KO* embryos; n = 3, $*P < 0.01$ compared to Wt. Original magnifications ×80 (**A** and **B**) and ×200 (**C**). Effects of *Ggnbp2KO* on cell proliferation in the E15.5 placentae (**E**–**J**). The proliferative nuclei (**E**–**I**, brown color) are visualized by BrdU immunohistochemical staining and counterstained by hematoxylin. There are more abundant BrdU-positive nuclei in the null mutant labyrinth (**F**, **H**, and **I**) compared to the Wt (**E** and **G**).The cells in the clusters in the null mutant labyrinth appear to be preferentially labeled with BrdU. There are no significant differences in proliferation of SpT cells or primary TGC between Wt and null mutant placentae (**E** and **F**). Quantitative morphometric analysis displays significant higher levels of BrdU incorporation in the *Ggnbp2KO* labyrinths than the Wt placentae (**J**). Original magnifications ×40 (**E** and **F**), ×100 (**G** and **H**), and ×200 (**I**); bar = 10 μm; n = 3, $*P < 0.01$ compared to Wt.

and C) in the junctional zone, while the immunostaining intensity in labyrinth TGCs was greater in E15.5 than E10.5 placentae (Fig. 2, D and E).

Ggnbp2KO *Results in a Dramatic Reduction of Vascular Spaces in the Labyrinth*

To further characterize the structural defects in the labyrinth of *Ggnbp2KO* placentae, the maternal and fetal interface were quantitatively analyzed by double labeling of alkaline phosphatase, a marker of SynT that surrounds maternal blood sinusoids, and laminin, a marker of fetal vascular endothelial cells (Fig. 3A). The results indicated that both maternal and fetal vascular spaces were dramatically reduced, while the labyrinth nonvessel area was markedly increased in the *Ggnbp2* null mutant placentae compared to Wt siblings (Fig. 3, A–D).

To determine whether the reduction of vascular spaces in the *Ggnbp2KO* labyrinth could be caused by an alteration of potential secretory factors produced by the placenta that affects angiogenesis, we tested the effect of conditioned medium from explant cultures of E15.5 placentae on HUVEC tube formation in vitro. There was not a significant difference in branch formation of HUVEC cultured in either Wt or mutant conditioned medium (Supplemental Fig. S2, A and B). These findings suggest that the reduction of vascular spaces in the *Ggnbp2KO* labyrinth is unlikely caused by an impairment of secretory factors produced by the placenta. Rather, it is possible that GGNBP2 may play a role in the intrinsic ability of endothelial or progenitor cells to form vascular networks.

Ggnbp2KO *Leads to an Increase in Trophoblast Proliferation in the Labyrinth*

To determine whether a compact labyrinth in *Ggnbp2* null placenta was caused by overcellular expansion or a decrease in apoptosis, or both, we performed BrdU and TUNEL assays. The labyrinth of *Ggnbp2KO* E15.5 placentae displayed a remarkable increase in the number of cells undergoing division (Fig. 3, E–J), especially the cells in the clusters. TUNEL

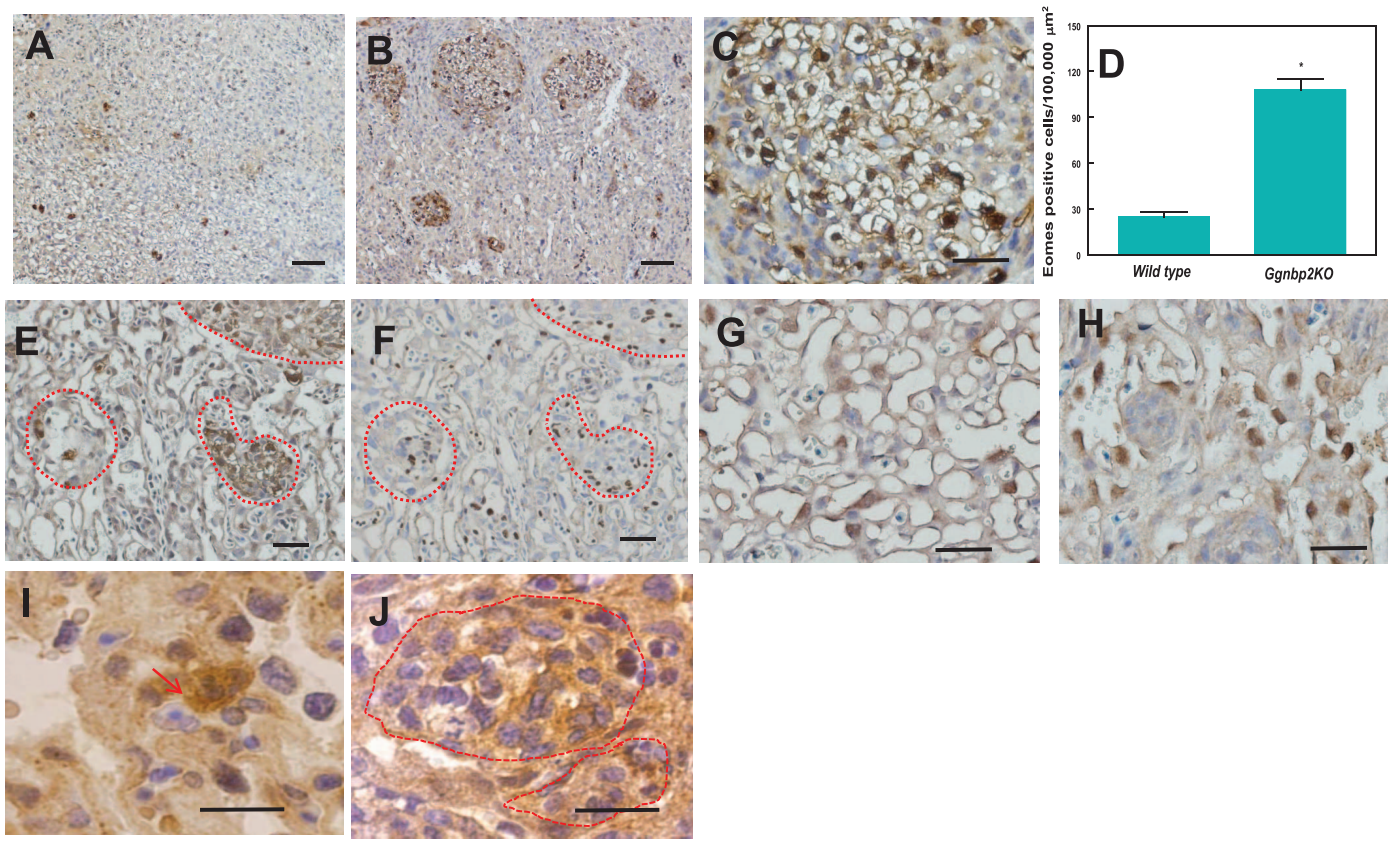

FIG. 4. Immunohistochemical staining of a trophoblast stem cell (TSC) marker Eomes (**A**–**C**) indicates that more abundant Eomes (**B** and **C**) in the *Ggnbp2KO* E15.5 labyrinths than the Wt placentae (**A**). The majority of Eomes-positive cells are observed in the clusters of the null mutant labyrinths (**B** and **C**). Quantitative morphometric analysis shows that null mutant placentae have significant higher levels of Eomes (**D**). Immunostaining of adjacent sections of null mutant E15.5 placentae for Eomes (**E**) and BrdU (**F**) shows that some but not all Eomes-positive cells in the clusters (outlined by red dashed lines) are labeled with BrdU. TGCs are immunostained positively for Hand 1 in Wt (**G**) and null mutant E15.5 labyrinths (**H**), but Hand 1-positive cells in the clusters of mutant labyrinths are not observed (**H**). Immunohistochemistry demonstrated that only a few cells in Wt E15.5 placentae were stained by a trophoblast progenitor cell marker Epcam (red arrow in **I**), but most of the cells in the clusters of the *Ggnbp2KO* E15.5 labyrinths (**J**) are stained positively for Epcam (outlined by red dashed lines). All the sections are counterstained with hematoxylin to visualize the cell nuclei. $*P < 0.01$ (**D**) compared to Wt, n = 3. Original magnifications ×40 (**A** and **B**), ×100 (**E** and **F**), ×200 (**C**, **G**, and **H**), and ×400 (**I** and **J**). Bar = 10 μm.

assays, on the other hand, did not exhibit a significant difference between Wt and mutant placentae (Supplemental Fig. S2, C and D).

Accumulation of TSCs in the Ggnbp2KO *Labyrinth*

To investigate which cell types were in these clusters in the *Ggnbp2KO* labyrinth, we carried out serial sectioning of E15.5 placentae and immunostained adjacent sections for BrdU and Eomes (a marker of TSCs). Quite a few cells in the clusters were labeled by both BrdU and Eomes. These observations suggested that these cell clusters likely were aggregates of TSCs and trophoblast progenitors, and implicated a potential increase in TSC self-renewal and a delay in their differentiation in the *Ggnbp2*-deficient labyrinth. As shown in Figure 4, not all cells in the clusters were Eomes positive and BrdU labeled. None of the cells in the clusters were positive for Hand 1, but most of the cells were stained by Epcam. It is possible that in addition to TSCs, the clusters within the labyrinth also contained certain types of trophoblast precursors such as SpT and glycogen cells or other cell types such as endothelial cells [29].

Ggnbp2KO *Overactivates Src and Stat3 in the Placenta*

To elucidate the potential signaling mechanisms involved in aberrant trophoblast proliferation and differentiation in the *Ggnbp2KO* labyrinth, we used Western blots to screen the phosphorylation status of several signal transducers and effectors. Surprisingly, the phosphorylation of Src (a non-receptor tyrosine kinase) and Stat3 in mutant placentae was markedly elevated (Fig. 5A), while the phosphorylation of other Stat transcription factors, the molecules that associate with PI3K (phosphoinositide 3-kinase), MAPK (mitogen-activated protein kinase), and mTOR (mammalian target of rapamycin) pathways were not significantly changed (Fig. 5B). The increase in phosphorylation of Src was only detected in tyrosine 416 but not tyrosine 527. The phosphorylation of both tyrosine 705 and serine 727 of Stat3 were noticeably enhanced. These results corroborate the hypothesis that *Ggnbp2KO* caused an overactivation of both Src and Stat3 in the mutant placentae. It is worth noting that the total Src and Stat3 protein levels in *Ggnbp2KO* placentae did not significantly differ from Wt, suggesting that the Src and Stat3 gene expression in *Ggnbp2KO* placentae are unlikely affected. Although there were variations in the phosphorylation levels of several other Stats, such as Stat2, Stat5, and Stat6, the changes in *Ggnbp2* null placentae were not statistically significant compared to the Wt. Together, our data showed that deletion of *Ggnbp2* caused a remarkable increase of Src and Stat3 phosphorylation, but not other Stats, nor the total protein levels of Src and Stat3.

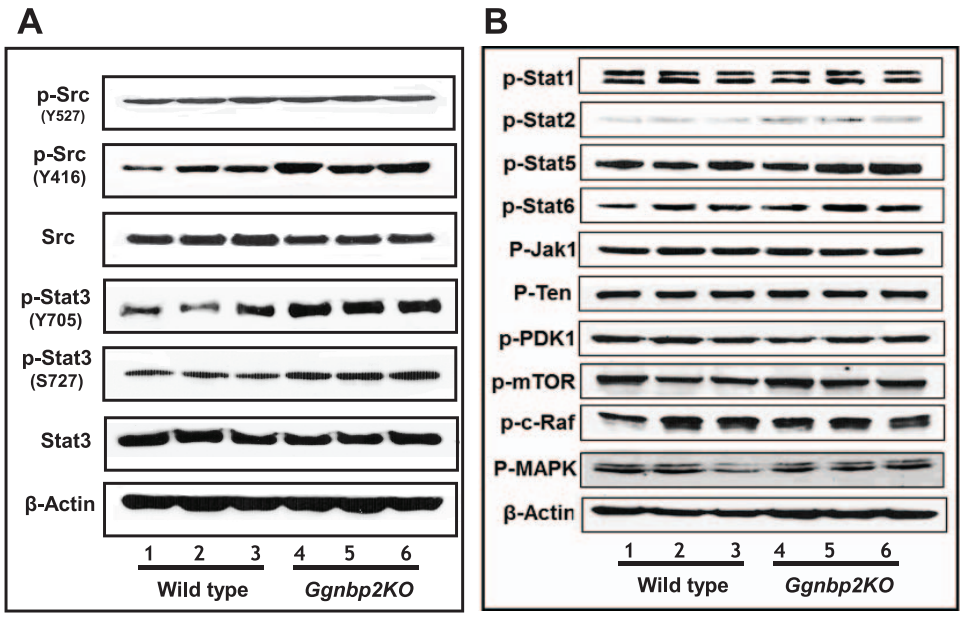

FIG. 5. **A**) Western blot analysis indicates that *Ggnbp2* deprivation enhances phosphorylated protein levels of Src and Stat3 in the E15.5 placentae. Semiquantitative analysis shows that there are 2.2-, 3.1-, and 1.9-fold increase in phosphorylation of Src (Y416), Stat3 (Y705), and Stat3 (S727) in the *Ggnbp2KO* placentae, respectively (n = 3). **B**) Western blots of E15.5 placenta protein show that the levels of phosphorylated Stat1, Stat2, Stat5, Stat6, Jak1, PDK1, mTOR, c-Raf, and MAPK are not significantly altered by *Ggnbp2* deletion.

Ggnbp2KO *Elevates the mRNA and Protein Levels and Phosphorylation of c-Met in the Labyrinth*

We next sought to determine the upstream signaling molecules that may be involved in Stat3 overactivation in the *Ggnbp2KO* labyrinth. Based on the information concerning GGNBP2's structure and nuclear localization, GGNBP2 likely functions as a transcription factor to regulate gene expression and/or interacts with other nuclear factors to modulate gene transcription. In the search for candidate genes that were affected by *Ggnbp2* ablation in the labyrinth, we focused on the family members of RTK and cytokines. The expression of the following genes in the E15.5 placentae were examined by RT-PCR: interleukin 6 (*Il6*), *Il6* receptor, leukemia inhibitory factor (*Lif*), Lif receptor, fibroblast growth factor 2 (*Fgf2*), *Fgf4, Fgf8*, *Fgf* receptor 1 (*Fgfr1*), *Fgfr2, Fgfr3, Fgfr4, Fgfr5,* epidermal growth factor (*Egf*), transforming growth factor-α, amphiregulin, betacellulin, epiregulin, *Egf* receptor, hepatocyte growth factor (*Hgf*), *c-Met,* platelet-derived growth factor-α (*Pdgfa*), *Pdgfb, Pdgf* receptor, vascular endothelial growth factor A (*Vegfa*), *Vegfb, Vegfc,* Vegf receptor 1 (*Vegfr1*), *Vegfr2,* and *Vegfr3*. We also checked the expression of hypoxia inducible factors *Hif1a* and *Hif1b*. Among these genes, a significant increase in *c-Met* mRNA levels was invariably detected (Fig. 6A; other data not shown). Moreover, Western blots showed significant elevations of total and phosphorylated c-Met protein levels in the *Ggnbp2KO* placentae (Fig. 6, B and C). Interestingly, immunofluorescent staining revealed that quite a few cells in these clusters in the *Ggnbp2KO* labyrinth contained high levels of phosphorylated c-Met protein (Fig. 6E). These results suggest that aberrant overactivation of the c-Met-Stat3 signaling pathway likely links to trophoblast hyperproliferation in the *Ggnbp2KO* labyrinth. This association is further corroborated by coincident up-regulation of *c-Myc* and *c-Fos* expression, the well characterized downstream target genes of c-Met signaling (Supplemental Fig. S3) [30–32].

Expression of c-Met *and C-Met and Stat3 Phosphorylation Associate with GGNBP2 Levels in TSCs*

To gain further understanding of the effect of GGNBP2 on the c-Met expression, a Wt TSC line derived from a C57BL/6 E3.5 blastocyst was established (Supplemental Fig. S4). The properties of TSCs were verified by continuous proliferation culture in MEF conditioned medium plus FGF4 (Supplemental Fig. S4) and expression of TSC markers, such as *Cdx2* and *Esrrb* (data not shown). TSCs spontaneously differentiated into TGCs in the absence of MEF conditioned medium and FGF4 (Supplemental Fig. S4) and expressed TGC markers, including cytokeratin (Supplemental Fig. S4), *Pl-1, Prl2c2,* and *Tpbpa* (data not shown). To test the effect of GGNBP2 on the expression of *c-Met, Ggnbp2* in TSCs was either overexpressed by stable transfection of an expression vector carrying a full length of mouse *Ggnbp2* cDNA or knocked down by *shRNA* interference. The results revealed that *Ggnbp2* overexpression in mouse TSCs significantly down-regulated *c-Met* mRNA (data not shown) and both total and phosphorylated c-Met protein levels (Fig. 7A), while suppression of *Ggnbp2,* on the other hand, remarkably up-regulated *c-Met* expression (data not shown) and its activation (Fig. 7B). Additionally, the phosphorylation of Stat3 in *Ggnbp2* overexpressed or knockdown TSCs was altered in parallel with the changes of *c-Met* expression and activation (Fig. 7B).

TSC Proliferation and Differentiation Are Inversely Affected by GGNBP2

To obtain evidence that GGNBP2 directly influences TSC proliferation, cell proliferation assays were carried out using these genetically manipulated TSCs. We found that there was a significant inhibition in cell proliferation when *Ggnbp2* was overexpressed in TSCs. In contrast, cell proliferation was noticeably stimulated when *Ggnbp2* was deliberately depleted (Fig. 7C). Moreover, the stimulation of cell proliferation in

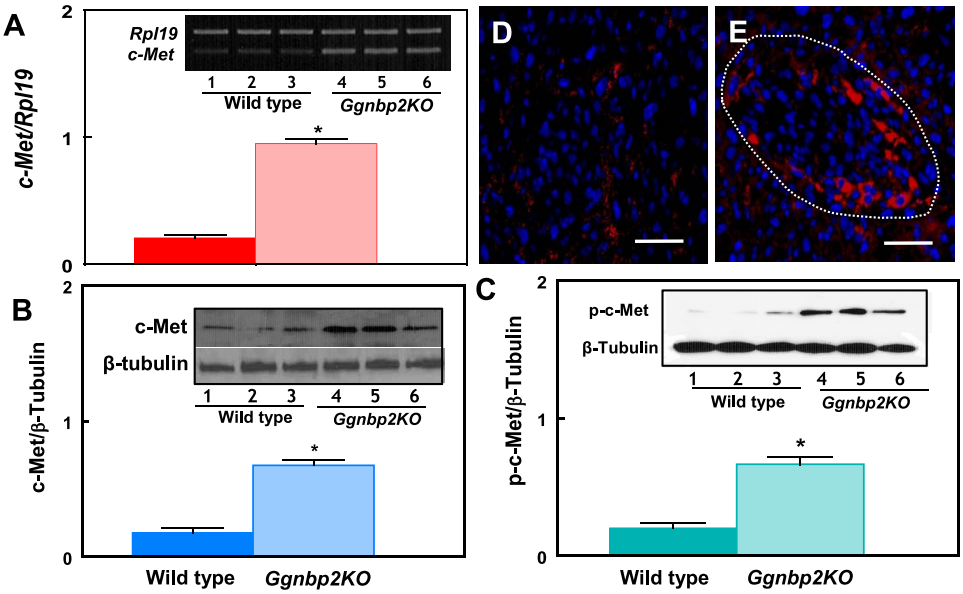

FIG. 6. *Ggnbp2KO* alters the expression of *c-Met* in the E15.5 placentae. The mRNA levels of *c-Met* (**A**) are determined by RT-PCR. The nonphosphorylated (**B**) and phosphorylated (**C**) protein levels of c-Met are detected by Western blot analysis. **D** and **E**) Representative pictures of immunofluorescent staining of phosphorylated c-Met (red color) in Wt (**D**) and the *Ggnbp2KO* (**E**) placentae. The contour of a cell cluster in the null mutant labyrinth is sketched by a white dashed line showing most of the phosphorylated c-Met-positive cells in the cluster. Cell nuclei are stained by 4′,6-diamidino-2-phenylindole (blue color). Original magnification ×400 (**D** and **E**); n = 3, $^*P < 0.01$ compared to Wt.

Ggnbp2-depleted TSCs was attenuated when these cells were treated with a Stat3-specific inhibitor WP1066 (Fig. 7D).

We further examined whether GGNBP2 affects TSC differentiation. Remarkably, we detected an inverted dependency of GGNBP2 levels on TSC proliferation and differentiation (Fig. 8). Using RT-PCR to determine the expression of TSC markers *Cdx2* and *Errb* and trophoblast markers *Pl-2, Prl2c2,* and *Tpbpa* when TSCs were cultured in differentiation medium, the results showed that the appearance of trophoblast markers and the disappearance of TSC markers were delayed in *Ggnbp2*-deficient TSCs. In contrast to these *Ggnbp2* knockdown TSCs, overexpression of *Ggnbp2* accelerated TSC differentiation into trophoblasts (Fig. 8).

DISCUSSION

In order to elucidate the function of *Ggnbp2* gene in mammalian physiology, we generated mice with targeted *Ggnbp2* inactivation in the C57BL/6 background. Surprisingly, null mutant embryos invariably die at late gestation, between E13.5 and E15.5, indicating that GGNBP2 is essential for fetal development. Analysis of *Ggnbp2* null mutant fetuses and placentae disclosed obvious defective placental development at the level of the labyrinthine zone, consistent with the high levels of GGNBP2 in this tissue. It appears to accumulate particularly in the nuclei of TGCs in the labyrinth during mid- to late gestation. The labyrinth layer is the functional interface critical for metabolic exchanges between the mother and fetus through direct contact of maternal blood lacunae and fetal blood vessels. Overexpanded nonvascular cell nests at the expense of maternal and fetal vascular spaces in the labyrinth layer leading to placental transport insufficiency appears to be the reason for the death of *Ggnbp2* null fetuses, although other causes such as undefined fetal abnormalities cannot be absolutely eliminated.

It is known that TSCs give rise to different types of trophoblasts in the labyrinth through a three-step process, that is, TSC exiting from cell cycle, transitional intermediate progenitors, and terminally differentiated trophoblasts, for example, TGC, SpT, and SynT. At the same time, TSCs are also undergoing self-renewal to maintain a proper size stem cell pool [12, 14, 33–36]. The most overt effect of the GGNBP2 absence on the labyrinth layer is an increase in the relative proportion of tissue occupied by TSC nests with hyperproliferative characteristic, suggesting that GGNBP2 may be important in controlling TSC decisions to expand or to differentiate. Functionally, GGNBP2 has been only examined previously in three studies conducted in vitro [22, 24, 25]. Forced expression of *LCRG1,* a short form of human *GGNBP2,* in Hela cells suppressed the proliferation, while knockdown of *LCRG1* by small interfering RNA promoted multiplication [22, 25]. Our in vivo investigation of the effects of *Ggnbp2KO* in the placenta is congruent with these two reports with respect to the role of GGNBP2 influencing cell proliferation. Intriguingly, a recent study reported that down-regulation of the long form of human *GGNBP2* by shRNA but not the short form in Hela cells resulted in a repression of cell proliferation, suggesting that the different isoforms of human *GGNBP2* might play different roles in the regulation of cell proliferation [24]. In this respect, it would be interesting to determine in future studies whether there is an isoform-dependent effect of GGNBP2 in vivo.

Many genes and signaling pathways have been implicated in the regulation of trophoblast homeostasis [9–11, 13, 37–39]. Our work unveils an important role of mammalian GGNBP2 in the modulation of trophoblast proliferation and differentiation. The present study reveals that constitutive overactivation of Stat3 in *Ggnbp2* null trophoblasts is accompanied by the phenotype of hyperproliferation and accumulation of TSCs in the labyrinth. In vitro genetic studies demonstrate that Stat3 activity is inversely associated with GGNBP2 levels. Furthermore, the pharmacological inhibitor of Stat3, WP1066, which specifically blocks phosphorylation, attenuates cell proliferation in *Ggnbp2* knockdown TSCs in a manner resembling *Ggnbp2* overexpression. Stat3 is known as a master regulator in the maintenance of stem cell renewal and stem state.

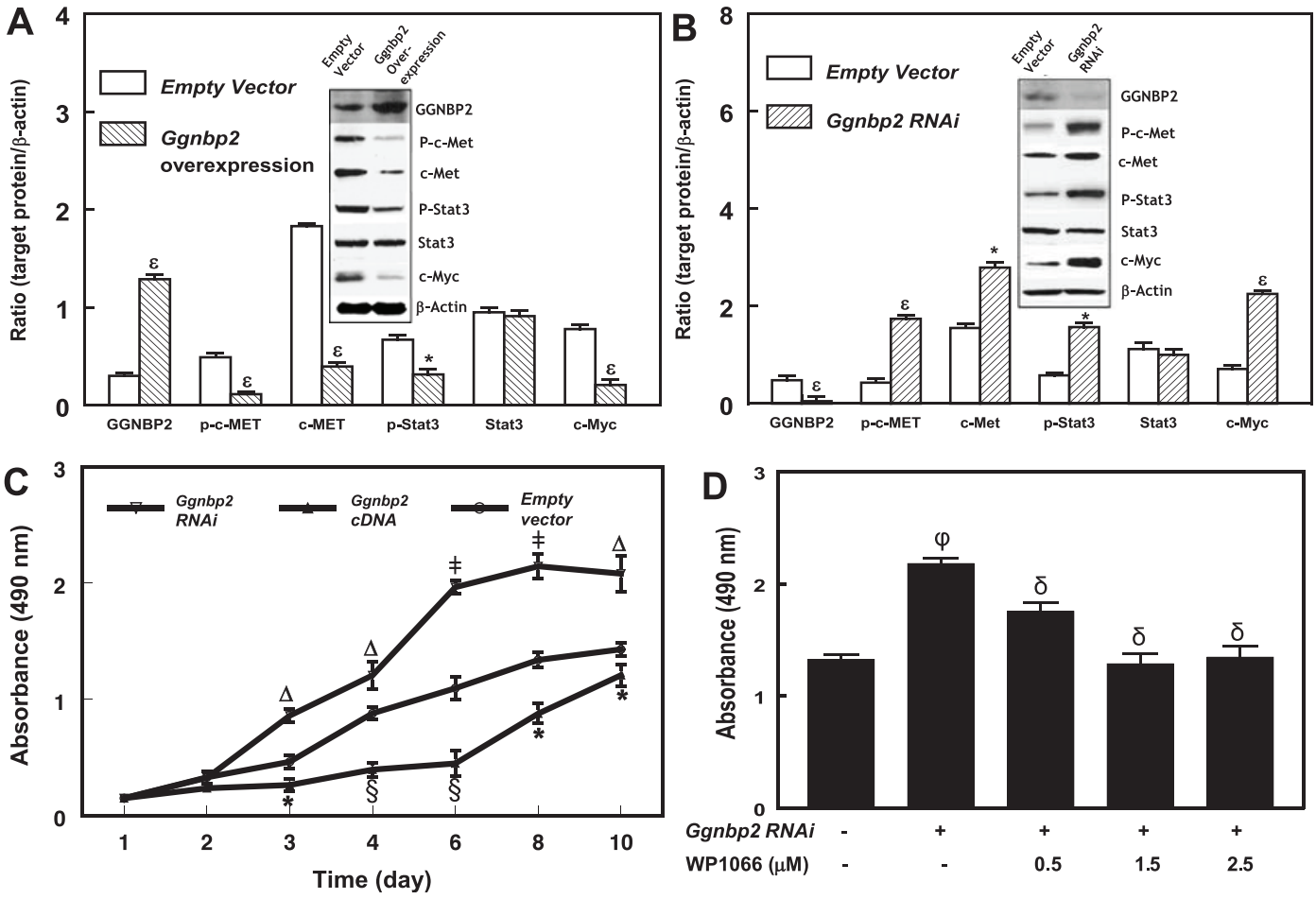

FIG. 7. GGNBP2-dependent *c-Met* expression and Stat3 phosphorylation in TSCs. GGNBP2 protein (**A**) levels are significantly increased in *Ggnbp2* cDNA-transfected TSCs, and its levels in *Ggnbp2 shRNA interference* lentiviral-transduced TSCs (**B**) are remarkably reduced as compared to the empty vector-transduced control TSCs. Western blot analyses reveal that c-Met expression and Stat3 phosphorylation are inversely correlated with *Ggnbp2* expression in TSCs (**A** and **B**). **C**) Effects of GGNBP2 on TSC proliferation in vitro. Cell proliferation is measured by the MTS-based assay method. The results reveal that *Ggnbp2* overexpression (▲) inhibits whereas *Ggnbp2* knockdown (▼) stimulates TSC proliferation compared to empty vector-transfected control TSCs (○). **D**) The enhanced cell proliferation in *Ggnbp2* knockdown TSCs is noticeably attenuated by an additional WP1066, a Stat3-specific inhibitor; n = 8, $^{\Delta}$ and $^{*}P < 0.05$ and $^{\ddagger, \varepsilon}$ and $^{\S}P < 0.01$ compared to control TSCs; $^{\varphi}P < 0.05$ compared to control TSCs; $^{\delta}P < 0.05$ compared to *Ggnbp2* RNA interference-transduced TSCs.

Overactivation of Stat3 has been shown to prevent stem cell differentiation [40–43]. Thus, we propose that hyperproliferation and accumulation of TSCs in the *Ggnbp2KO* labyrinth is likely caused by overactivation of Stat3 signaling.

Stat3 activation is marked by the phosphorylation of the tyrosine (Y705) and serine (S727) residues in cells primarily receiving signals from the RTK family [44–47]. In an initial attempt to determine the possible link between *Ggnbp2* loss and Stat3 overactivation in the placenta, we find that *c-Met* mRNA levels, among the other members of the RTK family examined, are significantly elevated in the *Ggnbp2KO* labyrinth. Functionally significant c-Met signaling has been extensively demonstrated in both physiological and pathological situations [15, 16, 48, 49]. Phosphorylation of c-Met activates several downstream signaling pathways, such as Src-Stat3, PI3K-PDK1 and Raf-MAPK cascades [18, 19]. The expression of a number of downstream target genes is affected in response to c-Met activation. For instance, a well characterized target gene, c-Myc is a key factor in maintaining the undifferentiated state and the self-renewal of ESCs [16, 19, 32, 48, 50]. Although there is no report so far regarding the effect of c-Met overactivation on placental development, it is known that high levels of c-Met expression and constitutive activation in several human cancers provoke uncontrolled cell expansion and malignant aggression [49, 51–54]. Our present data disclose that c-Met phosphorylation, its downstream effectors Src and Stat3, and target gene c-Myc are increased coincidently with a trophoblast hyperproliferation in the *Ggnbp2*-deficient placenta. Moreover, activation of c-Met and Stat3 is closely associated with the levels of GGNBP2. In vitro studies demonstrate that c-Met and Stat3 phosphorylation and TSC proliferation are elevated but TSC terminal differentiation are delayed when *Ggnbp2* is suppressed. In contrast, when *Ggnbp2* is overexpressed, completely opposite effects are observed. Thus, anomalous overactivation of a c-Met-Stat3 cascade in *Ggnbp2*-deprived placenta is, at least in part, attributable to malformation of the labyrinth through the perturbation of TSC proliferation and differentiation.

Experimental evidence emanating from previous studies suggests that overexpression of the *c-Met* gene is mainly due to aberrant transcriptional regulation [55]. Our data reveal that both *c-Met* mRNA and protein levels are increased in *Ggnbp2* null placentae. Bioinformatic analysis of GGNBP2 structure indicates that the protein contains a zinc finger and a nuclear receptor binding motif [20]. Immunostaining and ectopic expression experiments reveal that GGNBP2 protein is

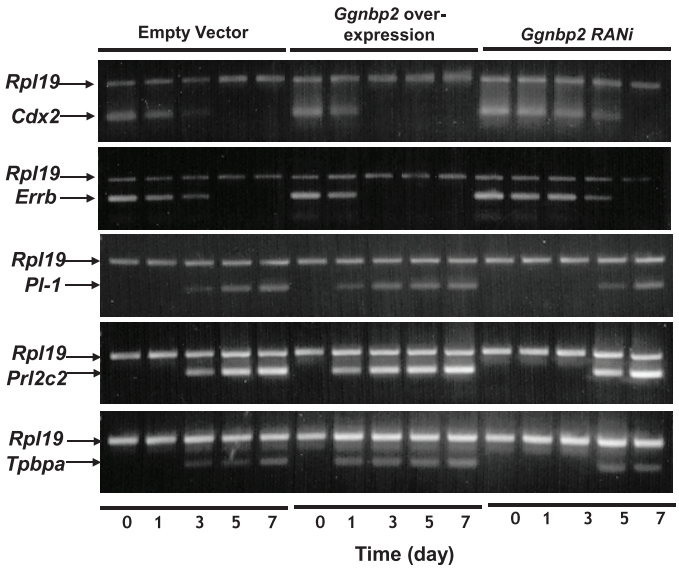

FIG. 8. Effects of GGNBP2 on TSC differentiation in vitro. RNA from control TSCs (empty vector), *Ggnbp2* overexpression, and *Ggnbp2* knockdown (*Ggnbp2 RNA interference*) in differentiation media at indicated times are analyzed by RT-PCR for the expression of TSC markers *Cdx2* and *Errb* and differentiated trophoblast markers *Pl-1, Prl2c2,* and *Tpbpa*.

localized in the nuclei [20, 22]. Our unpublished studies using electrophoretic mobility shift assay shows that GGNBP2 can directly bind double-stranded DNA. These data tempt us to speculate that GGNBP2 might normally function as a transcriptional repressor regulating *c-Met* gene expression in the placenta, yet the underlying mechanisms warrant further investigation.

Here, we uncover an unexpected role for GGNBP2 in the regulation of placental labyrinth development. Elevated *Ggnbp2* expression likely serves to repress TSC proliferation and promote TSC differentiation. Loss of *Ggnbp2* leads to uncontrolled TSC expansion and hampers TSC differentiation. It is likely that a dysregulated expression of *c-Met* in GGNBP2-deficient TSCs leading to an aberrant overactivation of Stat3 may disturb the TSC repertoire, which eventually impairs vascularization and forms a dysfunctional labyrinth. Taken together, our results suggest that an inhibitory effect of GGNBP2 is necessary to keep the activity of c-Met-Stat3 signaling pathway in check to ensure the timing and/or balance between proliferation and differentiation of TSCs during normal placental labyrinth development.

Placental deficiency can dramatically affect the health and viability of both the fetus and the mother [1, 56]. Both human and murine placentae are of the hemochorial type in which the trophoblast villi are in direct contact with the maternal blood [2, 10, 14]. Over the past decade, extensive evidence indicates that the molecular mechanisms that govern development of the placenta are quite conserved between mice and humans [1, 8, 10]. Our preliminary studies demonstrate that normal human placentae express GGNBP2 in the trophoblasts throughout their entire gestation (data not shown). Therefore, discovery of the function of GGNBP2 in placentation and characterization of the cellular, signaling, and molecular mechanisms by which *Ggnbp2* deficiency leads to a malformation of the labyrinth in mice will provide additional insights into the normal placental development in humans. Conditions related to the over- and underdevelopment of trophoblasts may be relevant targets to further study the role of GGNBP2 in human placentae, including hypertensive disorders of pregnancy, intrauterine growth restriction, invasive placentation, and late trimester demise.

ACKNOWLEDGMENT

The authors are thankful for Ms. Robin J. Lawrence's helpful advice in the preparation and editing of this manuscript.

REFERENCES

1. Maltepe E, Bakardjiev AI, Fisher SJ. The placenta: transcriptional, epigenetic, and physiological integration during development. J Clin Invest 2010; 120:1016–1025.
2. Watson ED, Cross JC. Development of structures and transport functions in the mouse placenta. Physiology (Bethesda) 2005; 20:180–193.
3. Simmons DG, Natale DR, Begay V, Hughes M, Leutz A, Cross JC. Early patterning of the chorion leads to the trilaminar trophoblast cell structure in the placental labyrinth. Development 2008; 135:2083–2091.
4. Cross JC, Hemberger M, Lu Y, Nozaki T, Whiteley K, Masutani M, Adamson SL. Trophoblast functions, angiogenesis and remodeling of the maternal vasculature in the placenta. Mol Cell Endocrinol 2002; 187: 207–212.
5. Sferruzzi-Perri AN, Macpherson AM, Roberts CT, Robertson SA. Csf2 null mutation alters placental gene expression and trophoblast glycogen cell and giant cell abundance in mice. Biol Reprod 2009; 81:207–221.
6. Rossant J, Cross JC. Placental development: lessons from mouse mutants. Nat Rev Genet 2001; 2:538–548.
7. Kidder BL, Palmer S. Examination of transcriptional networks reveals an important role for TCFAP2C, SMARCA4, and EOMES in trophoblast stem cell maintenance. Genome Res 2010; 20:458–472.
8. El-Hashash AH, Warburton D, Kimber SJ. Genes and signals regulating murine trophoblast cell development. Mech Dev 2010; 127:1–20.
9. Latos PA, Hemberger M. Review: the transcriptional and signalling networks of mouse trophoblast stem cells. Placenta 2014; 35(Suppl): S81–S85.
10. Cross JC, Baczyk D, Dobric N, Hemberger M, Hughes M, Simmons DG, Yamamoto H, Kingdom JC. Genes, development and evolution of the placenta. Placenta 2003; 24:123–130.
11. Selesniemi KL, Reedy MA, Gultice AD, Brown TL. Identification of committed placental stem cell lines for studies of differentiation. Stem Cells Dev 2005; 14:535–547.
12. Hu D, Cross JC. Development and function of trophoblast giant cells in the rodent placenta. Int J Dev Biol 2010; 54:341–354.
13. Pfeffer PL, Pearton DJ. Trophoblast development. Reproduction 2012; 143:231–246.
14. Roberts RM, Fisher SJ. Trophoblast stem cells. Biol Reprod 2011; 84: 412–421.
15. Ueno M, Lee LK, Chhabra A, Kim YJ, Sasidharan R, Van Handel B, Wang Y, Kamata M, Kamran P, Sereti KI, Ardehali R, Jiang M, et al. c-Met-dependent multipotent labyrinth trophoblast progenitors establish placental exchange interface. Dev Cell 2013; 27:373–386.
16. Nakamura T, Sakai K, Nakamura T, Matsumoto K. Hepatocyte growth factor twenty years on: Much more than a growth factor. J Gastroenterol Hepatol 2011; 26(Suppl 1):188–202.
17. Dulak AM, Gubish CT, Stabile LP, Henry C, Siegfried JM. HGF-independent potentiation of EGFR action by c-Met. Oncogene 2011; 30: 3625–3635.
18. Corso S, Comoglio PM, Giordano S. Cancer therapy: can the challenge be MET? Trends Mol Med 2005; 11:284–292.
19. Trusolino L, Bertotti A, Comoglio PM. MET signalling: principles and functions in development, organ regeneration and cancer. Nat Rev Mol Cell Biol 2010; 11:834–848.
20. Ohbayashi T, Oikawa K, Iwata R, Kameta A, Evine K, Isobe T, Matsuda Y, Mimura J, Fujii-Kuriyama Y, Kuroda M, Mukai K. Dioxin induces a novel nuclear factor, DIF-3, that is implicated in spermatogenesis. FEBS Lett 2001; 508:341–344.
21. Stuart HT, van Oosten AL, Radzisheuskaya A, Martello G, Miller A, Dietmann S, Nichols J, Silva JC. NANOG amplifies STAT3 activation and they synergistically induce the naive pluripotent program. Curr Biol 2014; 24:340–346.
22. Zhang J, Wang Y, Zhou Y, Cao Z, Huang P, Lu B. Yeast two-hybrid screens imply that GGNBP1, GGNBP2 and OAZ3 are potential interaction partners of testicular germ cell-specific protein GGN1. FEBS Lett 2005; 579:559–566.
23. Zhang X, Xiao Z, Chen Z, Li C, Li J, Yanhui Y, Yang F, Yang Y, Oyang

Y. Comparative proteomics analysis of the proteins associated with laryngeal carcinoma-related gene 1. Laryngoscope 2006; 116:224–230.
24. Guan R, Wen XY, Wu J, Duan R, Cao H, Lam S, Hou D, Wang Y, Hu J, Chen Z. Knockdown of ZNF403 inhibits cell proliferation and induces G2/M arrest by modulating cell-cycle mediators. Mol Cell Biochem 2012; 365:211–222.
25. Duan CJ, Jiang TB, Li C. Screening the effective target sequences of laryngeal carcinoma related gene LCRG1 [in Chinese]. Zhong Nan Da Xue Xue Bao Yi Xue Ban 2008; 33:468–475.
26. Dupressoir A, Vernochet C, Bawa O, Harper F, Pierron G, Opolon P, Heidmann T. Syncytin-A knockout mice demonstrate the critical role in placentation of a fusogenic, endogenous retrovirus-derived, envelope gene. Proc Natl Acad Sci U S A 2009; 106:12127–12132.
27. Rodriguez TA, Sparrow DB, Scott AN, Withington SL, Preis JI, Michalicek J, Clements M, Tsang TE, Shioda T, Beddington RS, Dunwoodie SL. Cited1 is required in trophoblasts for placental development and for embryo growth and survival. Mol Cell Biol 2004; 24:228–244.
28. Chiu SY, Maruyama EO, Hsu W. Derivation of mouse trophoblast stem cells from blastocysts. J Vis Exp 2010; (40):1964.
29. Tunster SJ, Tycko B, John RM. The imprinted Phlda2 gene regulates extraembryonic energy stores. Mol Cell Biol 2010; 30:295–306.
30. Abounader R, Reznik T, Colantuoni C, Martinez-Murillo F, Rosen EM, Laterra J. Regulation of c-Met-dependent gene expression by PTEN. Oncogene 2004; 23:9173–9182.
31. Li Y, Guessous F, Johnson EB, Eberhart CG, Li XN, Shu Q, Fan S, Lal B, Laterra J, Schiff D, Abounader R. Functional and molecular interactions between the HGF/c-Met pathway and c-Myc in large-cell medulloblastoma. Lab Invest 2008; 88:98–111.
32. Li Y, Li A, Glas M, Lal B, Ying M, Sang Y, Xia S, Trageser D, Guerrero-Cazares H, Eberhart CG, Quinones-Hinojosa A, Scheffler B, et al. c-Met signaling induces a reprogramming network and supports the glioblastoma stem-like phenotype. Proc Natl Acad Sci U S A 2011; 108:9951–9956.
33. Simmons DG, Cross JC. Determinants of trophoblast lineage and cell subtype specification in the mouse placenta. Dev Biol 2005; 284:12–24.
34. Asanoma K, Kato H, Yamaguchi S, Shin CH, Liu ZP, Kato K, Inoue T, Miyanari Y, Yoshikawa K, Sonoda K, Fukushima K, Wake N. HOP/NECC1, a novel regulator of mouse trophoblast differentiation. J Biol Chem 2007; 282:24065–24074.
35. Odiatis C, Georgiades P. New insights for Ets2 function in trophoblast using lentivirus-mediated gene knockdown in trophoblast stem cells. Placenta 2010; 31:630–640.
36. Asanoma K, Kubota K, Chakraborty D, Renaud SJ, Wake N, Fukushima K, Soares MJ, Rumi MA. SATB homeobox proteins regulate trophoblast stem cell renewal and differentiation. J Biol Chem 2012; 287:2257–2268.
37. Hu D, Cross JC. Ablation of Tpbpa-positive trophoblast precursors leads to defects in maternal spiral artery remodeling in the mouse placenta. Dev Biol 2011; 358:231–239.
38. Seabrook JL, Cantlon JD, Cooney AJ, McWhorter EE, Fromme BA, Bouma GJ, Anthony RV, Winger QA. Role of LIN28A in mouse and human trophoblast cell differentiation. Biol Reprod 2013; 89:95.
39. Townley-Tilson WH, Wu Y, Ferguson JE III, Patterson C. The ubiquitin ligase ASB4 promotes trophoblast differentiation through the degradation of ID2. PLoS One 2014; 9:e89451.
40. Levy DE, Lee CK. What does Stat3 do? J Clin Invest 2002; 109: 1143–1148.
41. Yang J, van Oosten AL, Theunissen TW, Guo G, Silva JC, Smith A. Stat3 activation is limiting for reprogramming to ground state pluripotency. Cell Stem Cell 2010; 7:319–328.
42. Hirai H, Karian P, Kikyo N. Regulation of embryonic stem cell self-renewal and pluripotency by leukaemia inhibitory factor. Biochem J 2011; 438:11–23.
43. Guryanova OA, Wu Q, Cheng L, Lathia JD, Huang Z, Yang J, MacSwords J, Eyler CE, McLendon RE, Heddleston JM, Shou W, Hambardzumyan D, et al. Nonreceptor tyrosine kinase BMX maintains self-renewal and tumorigenic potential of glioblastoma stem cells by activating STAT3. Cancer Cell 2011; 19:498–511.
44. Levy DE, Darnell JE Jr. Stats: transcriptional control and biological impact. Nat Rev Mol Cell Biol 2002; 3:651–662.
45. Brivanlou AH, Darnell JE Jr. Signal transduction and the control of gene expression. Science 2002; 295:813–818.
46. O'Shea JJ, Gadina M, Schreiber RD. Cytokine signaling in 2002: new surprises in the Jak/Stat pathway. Cell 2002; 109(Suppl):S121–S131.
47. Silva CM. Role of STATs as downstream signal transducers in Src family kinase-mediated tumorigenesis. Oncogene 2004; 23:8017–8023.
48. Organ SL, Tsao MS. An overview of the c-MET signaling pathway. Ther Adv Med Oncol 2011; 3:S7–S19.
49. Barrow-McGee R, Kermorgant S. Met endosomal signalling: in the right place, at the right time. Int J Biochem Cell Biol 2014; 49:69–74.
50. Ohya W, Funakoshi H, Kurosawa T, Nakamura T. Hepatocyte growth factor (HGF) promotes oligodendrocyte progenitor cell proliferation and inhibits its differentiation during postnatal development in the rat. Brain Res 2007; 1147:51–65.
51. Qiao H, Hung W, Tremblay E, Wojcik J, Gui J, Ho J, Klassen J, Campling B, Elliott B. Constitutive activation of met kinase in non-small-cell lung carcinomas correlates with anchorage-independent cell survival. J Cell Biochem 2002; 86:665–677.
52. Bertotti A, Burbridge MF, Gastaldi S, Galimi F, Torti D, Medico E, Giordano S, Corso S, Rolland-Valognes G, Lockhart BP, Hickman JA, Comoglio PM, et al. Only a subset of Met-activated pathways are required to sustain oncogene addiction. Sci Signal 2009. 2:ra80.
53. Dai Y, Siemann DW. Constitutively active c-Met kinase in PC-3 cells is autocrine-independent and can be blocked by the Met kinase inhibitor BMS-777607. BMC Cancer 2012; 12:198.
54. Gastaldi S, Sassi F, Accornero P, Torti D, Galimi F, Migliardi G, Molyneux G, Perera T, Comoglio PM, Boccaccio C, Smalley MJ, Bertotti A, et al. Met signaling regulates growth, repopulating potential and basal cell-fate commitment of mammary luminal progenitors: implications for basal-like breast cancer. Oncogene 2013; 32:1428–1440.
55. Ponzetto C, Giordano S, Peverali F, Della Valle G, Abate ML, Vaula G, Comoglio PM. c-met is amplified but not mutated in a cell line with an activated met tyrosine kinase. Oncogene 1991; 6:553–559.
56. Jansson T, Myatt L, Powell TL. The role of trophoblast nutrient and ion transporters in the development of pregnancy complications and adult disease. Curr Vasc Pharmacol 2009; 7:521–533.